

Correlating Acupuncture fMRI in the Human Brainstem with Heart Rate Variability

Vitaly Napadow, *Member IEEE*, Dhond RP, Purdon P, Kettner N, Makris N, Kwong KK, and Hui KKS

Abstract— Past neuroimaging studies of acupuncture have demonstrated variable results for important brainstem nuclei. We have employed cardiac-gated fMRI with T1-variability correction to study the processing of acupuncture by the human brain. Furthermore, our imaging experiments collected simultaneous ECG data in order to correlate heart rate variability (HRV) with fMRI signal intensity. Subjects experienced one of three stimulations over a 31.5 minute fMRI run: (1) electro-acupuncture at 2Hz/15Hz over the acupoint ST-36 (2) electro-acupuncture at a sham non-acupoint, or (3) sensory control tapping over ST-36. The ECG was analyzed with power spectral methods for low frequency and high frequency components, which reflect the balance in the autonomic nervous system. The HRV data was then correlated with the time-varying fMRI signal intensity. Our data suggests that fMRI activity in the hypothalamus, the dorsal raphe nucleus, the periaqueductal gray, and the rostral ventral medulla showed significant correlation with LF/HF ratio calculated from simultaneous HRV data. The correlation of time-varying fMRI response with physiological parameters may provide insight into connections between acupuncture modulation of the autonomic nervous system and neuroprocessing.

I. INTRODUCTION

Our group has been among the first to apply functional MRI to monitor the effects of acupuncture at some of the most frequently used classical acupuncture points [1-3]. Other investigators have also contributed [4-6], but the field of acupuncture neuroimaging is still in its infancy and much work remains. Most previous acupuncture fMRI investigations have incorporated a *short term* (<15min) block paradigm design; however, evidence from acupuncture analgesia studies suggests that a delayed response to acupuncture exists [7]. Thus, motivation

exists for performing longer duration (>30min) neuroimaging experiments.

Heart rate variability (HRV) analysis has been applied to indirectly monitor changes in sympathetic and parasympathetic balance. While some controversy in interpretation remains, the low frequency component (0.01-0.09Hz) is thought to predominantly reflect sympathetic activity, while the high frequency component (0.1-0.4Hz) reflects parasympathetic activity [8, 9]. Studies incorporating measures of autonomic nervous system (ANS) activity, including HRV, have demonstrated modulation by acupuncture [10-12]. Yao et al. demonstrated that acupuncture stimulation on rats produces a temporary increase in sympathetic tone, followed by a more prolonged depression [13]. Thus, ANS modulation may have temporal variability during acupuncture stimulation and may even correlate with the acupuncture induced activity in the brain, particularly the ANS centers of the subcortical gray and brainstem.

Past acupuncture fMRI studies have noted brainstem activation or deactivation [3, 14], but no consensus has been reached. Variability in brainstem activation may be due to short experiment runs, or to the existence of cardiogenic pulsatile motion artifact in the cerebrum and lower brain structures. Brainstem motion is chiefly along the cranio-caudal axis with total displacement on the order of 2-3mm [15], and is characterized by rapid displacement in systole (2mm/sec), followed by a slow diastolic recovery [16]. Velocity increases with caudal distance away from the cerebrum, as cervical spinal cord velocities have been estimated as high as 7.0mm/sec, [17]. Cardiac-gating the fMRI scan limits this motion artifact, though it produces fMRI data with variable repetition time (TR), and hence variable T1-weighting which must be corrected before any post-processing is applied. In this study, acupuncture effects in the human brainstem were evaluated by gating image acquisition to cardiac activity. We then correlated this fMRI activity with simultaneously derived HRV parameters.

II. METHODS

This study was performed on five (5) healthy, acupuncture naïve, right-handed (Edinburgh Inventory [18]) subjects (age: 21-33years). This study was approved by the Massachusetts General Hospital Subcommittee on Human Studies. Subjects were tested over two sessions (at least 48 hours apart), each with at most two 31.5 minute fMRI scans.

Subjects were outfitted with nasal cannula (in order to measure respiratory rate) and four chest ECG electrodes, and were asked to lie supine on the scanner bed, with eyes closed and attention focused on the needle site during experimental runs. Electrocardiogram (ECG) and respiratory data were recorded at 200Hz (InVivo Magnitude CV, Invivo Research Inc., Orlando, Florida) and fMRI data were gated to the ECG trace, with cluster acquisition after every other R-wave. Subjects were told their brain would be scanned in response to different forms of acupuncture. Three different stimulations were adopted for this study. For verum acupuncture, electro-acupuncture was performed between ST-36 and a point 1 cm proximal along the Stomach meridian. Pure silver

Manuscript received June 15, 2005. This work was supported in part by the NCCAM, NIH (K01AT002166-01, P01AT002048-02).

V Napadow is with Massachusetts General Hospital, Department of Radiology, Boston, MA 02129 USA (phone: 617-724-3402; fax: 617-726-7422; e-mail: vitaly@nmr.mgh.harvard.edu).

RP Dhond is with Massachusetts General Hospital, Department of Radiology, Boston, MA 02129 USA (e-mail: polly@nmr.mgh.harvard.edu).

P Purdon is with Massachusetts General Hospital, Department of Anesthesiology, Boston, MA 02129 USA (e-mail: ppurdon@mit.edu).

N Kettner is with Logan College of Chiropractic, Dept. of Radiology, Chesterfield, MO 63006 USA (e-mail: norman.kettner@logan.edu).

N Makris is with Massachusetts General Hospital, Department of Neurology, Boston, MA 02129 USA (e-mail: nikos@nmr.mgh.harvard.edu).

KK Kwong is with Massachusetts General Hospital, Department of Radiology, Boston, MA 02129 USA (e-mail: kwong@nmr.mgh.harvard.edu).

KKS Hui is with Massachusetts General Hospital, Department of Radiology, Boston, MA 02129 USA (e-mail: hui@nmr.mgh.harvard.edu).

acupuncture needles (0.25mm diameter, 40mm length, Maeda Corporation, Japan) were used due to the high magnetic field, and were inserted to a depth of approximately 2-3cm. Current was delivered with a modified current-constant H.A.N.S. (Han's Acupoint Nerve Stimulator) LH202 (Neuroscience Research Center, Peking University, Beijing, China) and consisted of 2Hz biphasic square-wave pulses alternating with 15Hz biphasic square-wave pulses every 3 seconds. Sham acupuncture consisted of identical electrostimulation applied between two non-acupoints approximately 8cm above the proximal edge of the patella, on the midline of the leg. Finally, tactile somatosensory control stimulation was performed by tapping at 2Hz over ST-36 with a 5.88 von Frey monofilament. The order and laterality of stimulation was pseudo-randomized. No more than two forms of stimulation were performed during each session, and opposite legs were stimulated if there were two runs in one session. After each run, subjects were questioned as to their psychophysical reaction to the procedure. The 31.5 minute stimulus paradigm consisted of a 1.5 minute rest period followed by 15 blocks of 1 minute stimulation followed by 1 minute without stimulation (**Figure 1**).

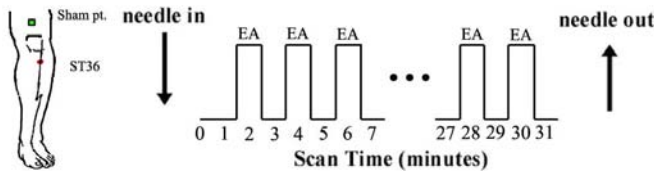


Fig. 1 – Acupoint ST-36 and a sham non-acupoint were stimulated during a 31.5min block design paradigm.

HRV Data Analysis

ECG data were acquired at 200Hz with laptop computer equipped with Labview 7.0 and DAQ card 6034E (National Instruments, Austin, TX) and processed with the WFDB (WaveForm DataBase) Software Package [19] and MATLAB 6.5 (The Mathworks, Inc. Natick, MA). Data were automatically annotated with careful manual correction in order to form an RR-interval time series. A power spectrum was then calculated using the multitaper method for 3 minute moving windows, offset by 1 minute intervals. LF and HF power were estimated by integrating within the 0.04-0.15Hz and 0.15-0.40Hz frequency bands, respectively. For subsequent regression analysis, normalized LF and HF power and LF/HF ratio were used.

MR Imaging Parameters

Functional and structural scans were acquired using a 3.0 Tesla Siemens Trio MRI System with an 8-channel head array coil equipped for echo planar imaging. One to two sets of structural images were collected prior to functional imaging using a T1-weighted MPRAGE sequence (TR/TE = 2.73/3.19ms, flip angle = 7°, FOV = 256x256mm; slice thickness = 1.33 mm) in order to facilitate visualization. BOLD functional imaging was performed using a gradient echo T2*-weighted pulse sequence (TE = 30msec, matrix = 64 x 64, FOV = 200mm, flip angle = 90°). Volume acquisition was gated to subjects' every other ECG R-wave; thus, TR varied with each acquisition (approximately 2sec). Cluster acquisition of 17 coronal slices was completed within 926ms (about a single RR-interval), 3mm thick with 0.6mm gap (voxel size 3.13 x 3.13 x 3mm). Motion correction was incorporated into the fMRI scanning sequence with Prospective Acquisition Correction (PACE, Siemens Medical Systems, Erlangen, Germany) – a critical addition due to the long duration scan runs.

Functional MRI Analysis

Images were first motion corrected with AFNI (NIH) through an iterated, linearized, weighted least-squares method with Fourier interpolation [20]. Data runs were excluded if gross translational motion exceeded 3mm on any axis. Data were then corrected for T1 variability (due to variable TR) using the method detailed by Guimaraes et al. [21]. Briefly, T1 was estimated by minimizing the variance in a fit of the exponential T1 decay curve and signal strength was corrected to a fixed TR value for each time point, avoiding spatial registration errors from any secondary datasets. No spatial or temporal pre-processing smoothing was done on the data as some brainstem nuclei are on the order of image voxel size. Statistical parametric mapping was completed via a generalized linear model (GLM) by first estimating the impulse response function from the input stimulus function (block design). The estimated response function was calculated separately for each of the 15 stimulation blocks. Each function was then compared with a partial F-test to the fMRI time series data and a general linear test was used to derive the partial F-statistic of the full model fit containing all 15 regressors (3dDeconvolve, AFNI). Thus, each on-block was free to demonstrate positive (activation), negative (deactivation), or no response to the stimulus - allowing for a time varying response of the BOLD signal in each voxel. The baseline was modeled with a 6th order Legendre polynomial due to the lengthy experimental run. Fit quality was measured by partial F-statistic (and associated p-value) and color-mapped onto the subject's own high resolution T1-weighted 3D anatomical dataset. Statistical regression analysis for each run was completed between HRV measures (LF, HF, LF/HF ratio) and percent signal change for the 15 different stimulation blocks by calculating the Pearson correlation coefficient and corresponding p-value (3dRegAna, AFNI).

III. RESULTS AND DISCUSSION

Our analysis suggests that certain areas of the brain contain time-varying response properties. For example, the rostral ventral medulla (RVM) demonstrated bimodal response to electroacupuncture at ST-36 – BOLD signal increase in the first 15 minutes of stimulation and BOLD signal decrease in the final 8 minutes of stimulation (**Figure 2**). This change in response suggests a time varying effect of acupuncture, which may underlie the necessity for longer (typically 30 minute) clinical acupuncture sessions.

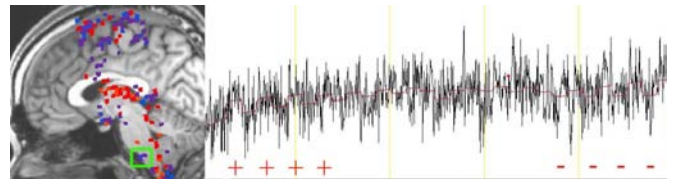


Fig 2 – The rostral ventral medulla (green box, Left) in a representative subject was activated in the first 15 minutes of stimulation, but was deactivated by the end of the 31.5min run. The full model fit is shown in red, overlaying the fMRI signal time course.

Long duration stimuli have been known to produce habituation in neuronal response, with decreasing numbers of neurons responding to a stimulus over time. This effect may be due to central attention mechanisms or to peripheral gating. We saw evidence of this behavior in the contralateral primary somatosensory cortex (SI), with a trend toward decreasing intensity of BOLD signal with time (**Figure 3**).

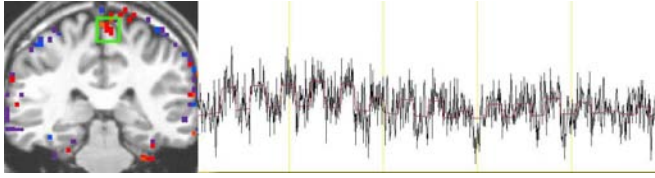


Figure 3 – The primary somatosensory area (green box, Left) in a representative subject demonstrated habituation– a decrease in the intensity of activation over the 31.5min run. The full model fit is shown in red, overlaying the fMRI signal time course.

Electro-acupuncture for a representative subject produced fMRI signal response that correlated with the HRV parameter LF/HF ratio in several key subcortical and brainstem structures. A positive correlation was seen in the hypothalamus. Both positive and negative correlations were seen in the RVM, while a negative correlation was seen in a midbrain region consistent with the dorsal raphe nucleus (DR) and the periaqueductal gray (PAG). Thus, when autonomic balance shifted towards the parasympathetic system (lower LF/HF ratio), activity in these midbrain regions was increased. Conversely, as autonomic balance shifted toward the sympathetic system (higher LF/HF ratio), activity in the hypothalamus was increased. The active area in the hypothalamus correlating with autonomic response was consistent with the dorsomedial (DMN) and paraventricular (PVN) nuclei. The PVN receives afferents from the rostral brainstem raphe nuclei and sends efferents to the motor nucleus of the vagus – thereby directly influencing autonomic control [22, 23]. Efferents from the DMN also connect with the PAG via the dorsal longitudinal fasciculus. The PAG, in turn, exerts its pain modulating action through the rostroventral medulla (RVM). The RVM includes the serotonergic raphe magnus nuclei and also receives inputs from the DR and hypothalamus [24]. Furthermore, the RVM includes On-cells, which facilitate nociception, and Off-cells which suppress it. These different classes of neurons in the RVM may explain why both positive and negative correlations were seen in the RVM, where stimulus blocks post 20 minutes demonstrated significant activation in some voxels (**Figure 4, Table 1**) and significant deactivation in others (**Figure 2**). While correlation does not infer causality, it is plausible that acupuncture modulation of the autonomic nervous system is an important component of its clinical efficacy. Thus modulation of the monoaminergic pathways (serotonin for DR) as well as the opioidergic pathway (PAG efferents to RVM) may prove important for clinical efficacy in a patient population.

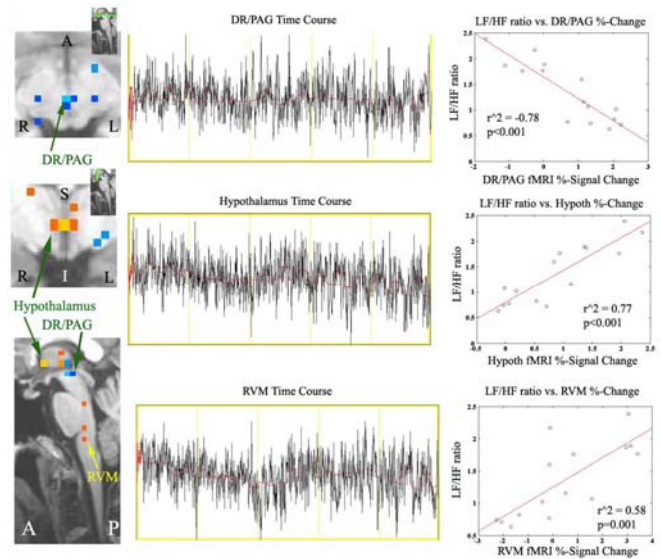


Fig. 4 – fMRI signal response correlated with the LF/HF ratio in three key structures of the brainstem. (n.b. RVM=rostroventral medulla, DR=dorsal raphe nucleus, PAG=periaqueductal gray, Hypoth=hypothalamus).

Structure	Talairach			-log (p)	r ² (w. LF/HF)
	x (mm)	y (mm)	z (mm)		
DR/PAG	0	-21	-4	7.24	-0.78
Hypothalamus	0	-2	-2	5.04	0.77
RVM	0	-34	-42	9.42	0.58

Table 1 – Summary table for correlated brain regions noted in Figure 4.

Acknowledgements

We would like to thank Wei Ting Zhang, Thomas Heldt, Greg Cavanagh, and Philipp Schroeder for helpful conversations in methods development.

REFERENCES

- Hui, K., et al. *Functional mapping of the human brain during acupuncture with magnetic resonance imaging*. in *Proceedings of 4th World Conference on Acupuncture*. 1996. New York.
- Hui, K.K., et al., *Acupuncture modulates the limbic system and subcortical gray structures of the human brain: evidence from fMRI studies in normal subjects*. *Hum Brain Mapp*, 2000. **9**(1): p. 13-25.
- Napadow, V., et al., *Effects of electroacupuncture versus manual acupuncture on the human brain as measured by fMRI*. *Hum Brain Mapp*, 2005. **24**(3): p. 193-205.
- Cho, Z.H., et al., *New findings of the correlation between acupoints and corresponding brain cortices using functional MRI*. *Proc Natl Acad Sci U S A*, 1998. **95**(5): p. 2670-3.
- Wu, M.T., et al., *Central nervous pathway for acupuncture stimulation: localization of processing with functional MR imaging of the brain--preliminary experience*. *Radiology*, 1999. **212**(1): p. 133-41.
- Wu, M.T., et al., *Neuronal specificity of acupuncture response: a fMRI study with electroacupuncture*. *Neuroimage*, 2002. **16**(4): p. 1028-37.
- Mayer, D., *Biological mechanisms of acupuncture*, in *Progress in Brain Research*, E. Mayer and C. Saper, Editors. 2000, Elsevier Science. p. 457-477.
- Task Force of the European Society of Cardiology, *Heart rate variability: standards of measurement, physiological interpretation and clinical use*. *Task Force of the European Society of Cardiology and the*

- North American Society of Pacing and Electrophysiology. *Circulation*, 1996. **93**(5): p. 1043-65.
9. Akselrod, S., et al., *Power spectrum analysis of heart rate fluctuation: a quantitative probe of beat-to-beat cardiovascular control*. *Science*, 1981. **213**(4504): p. 220-2.
 10. Cao, X.D., S.F. Xu, and W.X. Lu, *Inhibition of sympathetic nervous system by acupuncture*. *Acupunct Electrother Res*, 1983. **8**(1): p. 25-35.
 11. Haker, E., H. Egekvist, and P. Bjerring, *Effect of sensory stimulation (acupuncture) on sympathetic and parasympathetic activities in healthy subjects*. *J Auton Nerv Syst*, 2000. **79**(1): p. 52-9.
 12. Knardahl, S., et al., *Sympathetic nerve activity after acupuncture in humans*. *Pain*, 1998. **75**: p. 19-25.
 13. Yao, T., *Acupuncture and somatic nerve stimulation, mechanism underlying effects on cardiovascular and renal activities*. *Scand J Rehabil Med*, 1993. **29**: p. 7-18.
 14. Liu, W.C., et al., *fMRI study of acupuncture-induced periaqueductal gray activity in humans*. *Neuroreport*, 2004. **15**(12): p. 1937-40.
 15. Maier, S.E., C.J. Hardy, and F.A. Jolesz, *Brain and cerebrospinal fluid motion: real-time quantification with M-mode MR imaging*. *Radiology*, 1994. **193**(2): p. 477-83.
 16. Poncelet, B.P., et al., *Brain parenchyma motion: measurement with cine echo-planar MR imaging*. *Radiology*, 1992. **185**(3): p. 645-51.
 17. Mikulis, D.J., et al., *Oscillatory motion of the normal cervical spinal cord*. *Radiology*, 1994. **192**(1): p. 117-21.
 18. Oldfield, R.C., *The assessment and analysis of handedness: the Edinburgh inventory*. *Neuropsychologia*, 1971. **9**(1): p. 97-113.
 19. Goldberger, A.L., et al., *PhysioBank, PhysioToolkit, and PhysioNet: components of a new research resource for complex physiologic signals*. *Circulation*, 2000. **101**(23): p. E215-20.
 20. Cox, R.W., *AFNI: software for analysis and visualization of functional magnetic resonance neuroimages*. *Comput Biomed Res*, 1996. **29**(3): p. 162-73.
 21. Guimaraes, A.R., et al., *Imaging subcortical auditory activity in humans*. *Hum Brain Mapp*, 1998. **6**(1): p. 33-41.
 22. Parent, A., *Carpenter's Human Neuroanatomy*. 9th ed. 1996, Baltimore: Williams & Wilkins.
 23. Nilaver, G., et al., *Magnocellular hypothalamic projections to the lower brain stem and spinal cord of the rat. Immunocytochemical evidence for predominance of the oxytocin-neurophysin system compared to the vasopressin-neurophysin system*. *Neuroendocrinology*, 1980. **30**(3): p. 150-8.
 24. Fields, H. and A. Bussbaum, *Central nervous system mechanisms of pain modulation*, in *Textbook of Pain*, P. Wall and R. Melzack, Editors. 1999, Churchill Livingstone: New York.